

Ba incorporation in benthic foraminifera

Lennart J de Nooijer^{1*}, Anieke Brombacher^{2,a}, Antje Mewes³, Gerald Langer⁴, Gernot Nehrke³,
Jelle Bijma³, Gert-Jan Reichart^{1,2}

¹Royal Netherlands Institute of Sea Research, Dept of Ocean Sciences, Landsdiep 4, 1797 SZ
't Horntje, The Netherlands

*Corresponding author: ldenooijer@nioz.nl

²Utrecht University, Faculty of Geosciences, Budapestlaan 4, 3584 CD Utrecht, The
Netherlands

³Alfred-Wegener-Institut Helmholtz-Zentrum für Polar- und Meeresforschung, Biogeosciences
section, Am Handelshafen 12, 27570 Bremerhaven, Germany

⁴The Marine Biological Association of the United Kingdom, The Laboratory, Citadel Hill,
Plymouth, Devon, PL1 2PB, UK

^anow at: National Oceanography Centre, University of Southampton, Waterfront Campus,
European Way, Southampton SO14 3ZH, UK

Abstract

Barium (Ba) incorporated in the calcite of many foraminiferal species is proportional to the concentration of Ba in seawater. Since the open ocean concentration of Ba closely follows seawater alkalinity, foraminiferal Ba/Ca can be used to reconstruct the latter. Alternatively, Ba/Ca from foraminiferal shells can also be used to reconstruct salinity in coastal settings where seawater Ba concentration corresponds to salinity as rivers contain much more Ba than seawater. Incorporation of a number of minor and trace elements is known to vary (greatly) between foraminiferal species and application of element/Ca ratios thus requires the use of

26 species-specific calibrations. Here we show that calcite Ba/Ca correlates positively and linearly
27 with seawater Ba/Ca in cultured specimens of two species of benthic foraminifera,
28 *Heterostegina depressa* and *Amphistegina lessonii*. The slopes of the regression, however, vary
29 2-3 fold between these two species (0.33 and 0.78, respectively). This difference in Ba-
30 partitioning resembles the difference in partitioning of other elements (Mg, Sr, B, Li and Na)
31 in these foraminiferal taxa. A general trend across element partitioning for different species is
32 described, which may help developing new applications of trace elements in foraminiferal
33 calcite in reconstructing past seawater chemistry.

34

35 Keywords: foraminifera, Ba/Ca, proxies

36

37 **1 Introduction**

38 Incorporation of barium (Ba) in foraminiferal calcite is proportional to seawater barium
39 concentrations (e.g. Lea and Boyle, 1989; 1990; Lea and Spero, 1994). Open ocean surface
40 barium concentrations are relatively uniform (Chan et al., 1977; Broecker and Peng, 1982) and
41 since $[Ba^{2+}]$ is removed at the surface and regenerated at depth, its vertical concentration
42 resembles that of alkalinity (Li and Chan, 1979; Rubin et al., 2003). For this reason, fossil
43 foraminiferal Ba/Ca has been used to reconstruct past alkalinity (e.g. Lea, 1995). Locally,
44 seawater $[Ba^{2+}]$ can also reflect salinity due to the relatively high Ba/Ca of river- or meltwater
45 input (Hanor and Chan, 1977; Guay and Falkner, 1997; 1998) and therefore Ba/Ca in
46 foraminiferal calcite can be used to reconstruct paleosalinity (Hall and Chan, 2004b; Weldeab
47 et al., 2007; 2014; Bahr et al., 2013). These reconstructions can be complicated by upwelling
48 affecting surface Ba/Ca (Lea et al., 1989; Hatch et al., 2013). Moreover, Ba cycling at or close
49 to the seafloor can affect Ba uptake in benthic foraminifera (Ni Flaithearta et al., 2010).
50 Application of Ba/Ca critically depends on the prerequisite that temperature, salinity as such

51 (Lea and Spero, 1994; Hönisch et al., 2011) and photosymbiont activity (Lea and Spero, 1992;
52 Hönisch et al., 2011) do not affect Ba incorporation in foraminiferal shell carbonate. Still, Ba/Ca
53 ratios are known to vary within chamber walls of crust-producing planktonic foraminifera
54 (Eggins et al., 2003; Hathorne et al., 2009). Like Mg/Ca, the values for Ba in crust carbonate
55 are lower, which cannot be (solely) explained by migration to greater water depths during crust
56 formation (Hathorne et al., 2009). This argues for an unknown additional imprint on Ba
57 incorporation. On an intra-test scale, the distributions of Mg and Ba within the test wall of
58 *Pulleniatina obliquiloculata* have been shown to co-vary to some extent, with maximum
59 concentrations often, but not always, coinciding with the 'organic linings' (Kunioka et al.,
60 2006). For some other elements, including Mg and Sr, incorporation has been shown to be inter-
61 dependent (e.g. Mewes et al., 2015). Such interdependency, however, varies between pairs of
62 elements and is explained by a combination of simultaneous fractionation by the same process
63 (e.g. Langer et al., 2016) and by involvement of different processes during calcification (Nehrke
64 et al., 2013). These models and experimental results may imply that also the incorporation of
65 Ba could be influenced by these physiological processes and/ or the same fractionation process
66 during calcite precipitation (e.g. through lattice distortion; Mucci and Morse, 1983; Mewes et
67 al., 2015).

68 So far, Ba/Ca values have been reported for planktonic (Boyle, 1981; Lea and
69 Boyle, 1991; Lea and Spero, 1992; 1994; Hönisch et al., 2011; Marr et al., 2013; Hoffmann et
70 al., 2014) and low-Mg benthic species (Lea, 1995; Lea and Boyle, 1989; 1990; 1993; Reichart
71 et al., 2003). Although Mg/Ca is known to vary greatly between (benthic) foraminiferal species
72 (between ~1 and ~150 mmol/mol; Toyofuku et al., 2000; Bentov and Erez, 2006; Wit et al.,
73 2012) Ba/Ca, which is only rarely investigated in species producing high-Mg calcite (Evans et
74 al., 2015; Van Dijk et al., 2017). Ba/Ca in planktonic species may be used to reconstruct
75 (changes in) open ocean alkalinity (Lea, 1995), whereas those published for benthics may be

76 more suitable to reconstruct salinity in coastal and shelf seas (Weldeab et al., 2007; 2014; Bahr
77 et al., 2013). The range in Mg/Ca is known particularly for benthic foraminifera (e.g. Toyofuku
78 et al., 2011; Sadekov et al., 2014) and inter-species variability in Ba incorporation may therefore
79 hamper application of (benthic) foraminiferal Ba/Ca. Here we present results from a culture
80 study using the larger benthic foraminifera, *Amphistegina lessonii* and *Heterostegina depressa*,
81 two species with different Mg/Ca (~50 mmol/mol; Segev and Erez, 2006 and ~120 mmol/mol;
82 Dueñas-Bohórquez et al., 2011, respectively). In these culturing experiments, the range in
83 Ba/Ca exceeds the naturally occurring range in seawater to facilitate testing underlying controls
84 on barium incorporation. If there is a linear increase in shell Ba/Ca (Ba/Ca_{cc}) with increasing
85 seawater Ba/Ca (Ba/Ca_{sw}), the large range in Ba/Ca of the culturing media prepared here will
86 furthermore decrease uncertainty of the obtained Ba/Ca_{cc} - Ba/Ca_{sw} calibration. Our results are
87 compared to Ba/Ca in these species from field samples. Together, calibration of Ba/Ca in these
88 species against seawater Ba/Ca and in the context of other elemental incorporation data, allows
89 evaluation and application of incorporated Ba across a wider range of foraminiferal taxa, with
90 contrasting element composition of their shell.

91

92 **2 Methods**

93 *2.1 Culture media*

94 To determine Ba/Ca partitioning, benthic foraminiferal culture experiments were set up with
95 five different seawater Ba/Ca ratios (54-92 $\mu\text{mol/mol}$). Media were prepared by increasing
96 $[Ba^{2+}]_{sw}$ while keeping the $[Ca^{2+}]_{sw}$ constant. The range of $[Ba^{2+}]$ used in these experiments
97 exceeds the range of concentrations found naturally and allows testing the applicability of
98 partition coefficients under conditions with artificially high seawater Ba/Ca. Seawater is only
99 slightly undersaturated with respect to barite ($BaSO_4$) and an increase in $[Ba^{2+}]$ in the sea water
100 will cause barite precipitation (Langer et al., 2009). To be able to increase $[Ba^{2+}]$ beyond its

101 natural range, artificial seawater was prepared with lower sulphate contents. All other salts were
102 added according to the recipe of Kester et al. (1967) to produce a total of 5 litres of medium for
103 each treatment. As *Amphistegina lessonii* and *Heterostegina depressa* do not grow well in 100%
104 artificial seawater, the prepared media were mixed with natural seawater in a ratio 9:1 (Mewes
105 et al., 2014). To double check concentrations and determine potential loss of elements due to
106 precipitation, sorption and/or scavenging, element concentrations of the culture media were
107 determined by ICP-OES at the Alfred-Wegener-Institute in Bremerhaven, except for Ba which
108 was measured by ICP-MS at Utrecht University (Table 1).

109 Culture media pH was adjusted to 8.0 by adding NaOH (1 M) to the prepared media. Before
110 the start of the experiments, dissolved inorganic carbon (DIC) and total alkalinity were
111 measured at the Alfred-Wegener-Institute. DIC was measured photometrically in triplicates
112 with a TRAACS CS800 QuAAtro autoanalyser with an average reproducibility of $\pm 10 \mu\text{mol}$
113 L^{-1} . Alkalinity was calculated from linear Gran plots (Gran, 1952) after triplicate potentiometric
114 titration (Bradshaw et al., 1981) using a TitroLine alpha plus auto sampler (Schott
115 Instruments). Parameters of the total carbonate system were calculated from temperature,
116 salinity, DIC and alkalinity using the program CO2SYS (Lewis and Wallace, 1998) adapted to
117 Excel by (Pierrot et al., 2006). The equilibrium constants K1 and K2 from Mehrbach et al.
118 (1973), as reformulated by Dickson and Millero (1987) were used (Table 1).

119

120 2.2 Foraminiferal culturing

121 Living specimens of *A. lessonii* and *H. depressa* were isolated from sediment collected at the
122 tropical aquarium of Burger's Zoo (Arnhem, The Netherlands) in August 2012 and transferred
123 to the Alfred-Wegener-Institute for the culture experiments. Healthy individuals of *A. lessonii*
124 showing pseudopodial activity, a dark brown cytoplasm and minimal signs of bleaching were
125 handpicked with a small brush under a Zeiss Stereo microscope and transferred to well plates.

126 Adult specimens of *H. depressa* were picked directly from the aquarium with soft tweezers.
127 After two weeks several individuals of both species underwent asexual reproduction. Individual
128 *H. depressa* parent cells produced sufficient numbers of juveniles to study separate clone
129 groups. Approximately 20 juveniles with two or three chambers from the same parent were
130 selected for every treatment and divided over two Petri dishes (diameter 55 mm, containing
131 approximately 10 ml of culture medium). In total, two clone groups were used in the
132 experiments resulting in a total of at least 40 individuals per treatment. Specimens of *A. lessonii*
133 did not produce sufficient numbers of juveniles for analysis of separate clone groups. Therefore,
134 approximately 60 juveniles with two or three chambers from different parents were selected per
135 treatment and distributed evenly over three Petri dishes. All experiments were carried out in an
136 adjustable incubator (RUMED Rubarth Aparate GmbH) at a constant temperature of 25 °C. As
137 both species are symbiont-bearing, a 12:12 light:dark cycle was applied with a constant photon
138 flux density of approximately 250 $\mu\text{mol photons m}^{-2}\text{s}^{-1}$ during light hours. Pictures were taken
139 weekly under a Zeiss Axiovert 200M inverted microscope and maximal diameters of the shells
140 were measured with the AxioVision software to allow determining the chamber addition rates
141 of the foraminifera in the experiments. The experiments were terminated after six weeks.
142 All specimens were fed *Dunaliella salina* algae every three to four days. Although *A. lessonii*
143 hosts symbionts, this foraminiferal species does not exclusively rely on nutrients from their
144 symbionts, but also ingests algae (Lee, 2006). To avoid changes in the barium concentration of
145 the culture media, the water in the dishes containing foraminifera were diluted as little as
146 possible by the solution containing the food for the foraminifera. For this purpose, foraminifera
147 were fed 50 μl of a solution containing algae that was centrifuged at 2000 rpm for 10 minutes.
148 Algae concentrated at the bottom of the tube were transferred to an empty tube with a pipette.
149 To prevent changes in the culture media's carbonate chemistry by algal photosynthesis the algae
150 were killed by heating the concentrated solution in an oven at 90 °C for 10 minutes. The cultures

151 were transferred to new Petri dishes every week to avoid excessive bacterial growth, potential
152 build-up of waste products and shortage of ions or nutrients. To prevent changes in salinity by
153 evaporation media were refreshed three days after the cultures were transferred to new dishes
154 by pipetting approximately 5 ml of the old media out of the Petri dish and replacing it with the
155 same volume of media from the prepared batch.

156

157 *2.3 Sample preparation and analysis*

158 At the end of the culture experiment, specimens were cleaned by placing them in a 7% NaOCl
159 solution for approximately 30 minutes until completely bleached and organic material was
160 removed from the tests. This cleaning method is shown to have a similar impact on average
161 foraminiferal Ba/Ca values as cleaning with H₂O₂ and is relatively small (2-3 μmol/mol)
162 compared to cleaning with de-ionized water only (Pak et al., 2004). Specimens were then rinsed
163 three times for approximately 60 seconds in de-ionized water to remove the NaOCl and any
164 residual salts from the culture solutions. Cleaned foraminifera were put in an oven at 42 °C
165 until completely dry and mounted on sample holders using double sided adhesive tape.

166 Element composition of the calcite was determined using Laser Ablation-Inductively Coupled
167 Plasma-Mass Spectrometry (LA-ICP-MS) at Utrecht University (Reichert et al., 2003). The
168 system consisted of a Geolas 200Q 193 nm Excimer laser (Lambda Physik) connected to a
169 sector field-ICP-MS (Element2, Thermo Scientific). Samples were ablated in a single-volume
170 chamber and the aerosol was carried to the ICP-MS by a Helium flow. Monitored masses
171 included ²³Na, ²⁴Mg, ²⁶Mg, ²⁷Al, ⁴³Ca, ⁴⁴Ca, ⁵⁵Mn, ⁸⁸Sr, ¹³⁸Ba and ²³⁸U and calibration was
172 performed using a glass standard (NIST 610) that was ablated three times after every 10-12
173 foraminiferal samples. Diameter of the ablation crater was set to 80 μm for all specimens and
174 pulse repetition rate was 6 Hz. The ablated calcite was measured and integrated with respect to
175 time. Energy density for the glass was higher than for the foraminifera (5 J/cm² and 1 J/cm²,

176 respectively). Although the resulting difference in ablation characteristics is not likely to affect
177 obtained foraminiferal element concentrations (Hathorne et al., 2008), foraminiferal element
178 concentrations were compared to those from an in-house made calcite standard with known
179 element concentrations and ablated at the same energy density as the foraminifera (Dueñas-
180 Bohórquez et al., 2009). Relative standard deviation for Mg/Ca and Sr/Ca based on repeated
181 measurements on this material was <5% for both ratios. Due to the lamellar nature of Rotallid
182 foraminifera, final chambers are thinnest and are therefore characterized by largest uncertainty
183 in the estimated average element/Ca ratio. Therefore, the F chamber was not considered and
184 instead, the F-1 chamber of *A. lessonii* was ablated for every specimen. For *H. depressa*, walls
185 of the final two chambers were commonly too thin for reliable chemical results and, therefore,
186 the F-2 chamber was analysed. In addition, for each species, the final 6-7 chambers of ten
187 sufficiently large specimens (2 from each of the five treatments) were ablated to analyse intra-
188 specimen variability in Ba/Ca, to analyse variability within chamber walls as a function of
189 thickness and to detect potential ontogenetic trends in Ba incorporation.

190
191 Elemental concentrations were calculated from the ablation profiles with the Glitter software,
192 using ^{43}Ca as internal standard and values from Jochum et al. (2011) for concentrations of
193 elements in the NIST 610. This program integrates the ablation signal after subtracting the
194 background signal to calculate the elemental concentrations. To avoid contaminated intervals
195 of the ablation profile, sections with high ^{27}Al and ^{55}Mn counts were excluded from the analysis
196 since these parts are often also characterized by unusually high Mg/Ca not reflecting the actual
197 shell carbonate. Ablation profiles with a duration shorter than 5 seconds were rejected as such
198 short profiles are unreliable due to poor counting statistics. Nine out of 188 ablation profiles
199 were rejected for *A. lessonii* and 7 out of 140 profiles from *H. depressa* were discarded, which
200 is less than 5%.

201

202 2.4 Aquarium samples

203 To compare the results from cultured specimens with Ba/Ca from specimens derived from
204 'natural conditions', a number of living specimens of both *A. lessonii* and *H. depressa* were
205 isolated from the Zoo's stock (i.e. sediment collected at the zoo from which the specimens were
206 isolated; section 2.2) and cleaned and prepared for LA-ICP-MS analyses as described in 2.3.
207 From both species, 7 specimens were ablated twice at the Royal NIOZ using a NWR193UC
208 (New Wave Research) laser, containing an ArF Excimer laser (Existar) with deep UV 193 nm
209 wavelength and <4 ns pulse duration. Provided that the same reference material is used, the use
210 of multiple laser systems (see above) is shown not to bias obtained foraminiferal element/Ca
211 ratios (De Nooijer et al., 2014a). Laser ablation was performed with an energy density of 1
212 J/cm² at a repetition rate of 6 Hz for calcite samples and an energy density of 5 J/cm² for the
213 glass (NIST610) standards. Helium was used as a carrier gas with a flow rate of 0.8 L/min for
214 cell gas and 0.3 L/min for cup gas. From the laser chamber to the quadrupole ICP-MS (iCAP-
215 Q, Thermo Scientific), the He flow was mixed with ~0.4 L/min nebulizer Ar. Before measuring
216 the samples, the nebulizer gas, extraction lens, CCT focus lens and torch position were
217 automatically tuned for the highest sensitivity of ²⁵Mg by laser ablating MACS-3. The masses
218 measured by the ICP-MS were ²³Na, ²⁴Mg, ²⁵Mg, ²⁷Al, ⁴³Ca, ⁴⁴Ca, ⁸⁸Sr and ¹³⁸Ba. JcP-1,
219 MACS-3 and an in-house (foraminiferal) calcite standard (NFHS) were used for quality control
220 and measured every 10 foraminiferal samples. Internal reproducibility of the analyses was all
221 better than 9%, based on the three different carbonate standards used. Intensity data were
222 integrated, background subtracted, standardized internally to ⁴³Ca and calibrated against the
223 MACS-3 signal using a custom-built MATLAB routine within the program SILLS (Guillong
224 et al., 2008). Since ablation of the NIST SRM 610 and NIST SRM 612 could increase the
225 sodium background, they were only ablated and analyzed at the end of every sequence and

226 cones were cleaned before the next sequence. Accuracy of the analyses was better than 3%,
227 based on comparing the carbonate standards with internationally reported values (Okai et al.,
228 2002, Wilson et al., 2008). Signals were screened for surface contamination and parts of the
229 outside or inside of the shell with elevated Mg, Mn or Al values were eliminated from the area
230 selected for integration.

231 Seawater samples from the Zoo's aquarium were measured in duplicate using a sector field-
232 ICP-MS (Element2, Thermo Scientific). The ICP-MS was run in low resolution mode (24
233 cycles) for ^{138}Ba and in medium resolution (24 cycles) for ^{43}Ca . Calibration was performed
234 through an external calibration series with increasing concentrations of Ba.

235

236 **3 Results**

237 *3.1 Test diameter increase*

238 Average shell diameters increased considerably during the experimental period (Figure 1).
239 Overall, increase in shell diameter did not significantly differ between treatments. Treatment C
240 (seawater Ba/Ca = 64 $\mu\text{mol/mol}$) for *A. lessonii*, however, shows somewhat reduced chamber
241 addition rates per incubated specimen. This may be the consequence of slightly higher mortality
242 under these conditions and a relatively high number of specimens that did not add any
243 chambers. Although not systematically investigated, two Petri dishes from this treatment
244 contained relatively many bleached (i.e. devoid of symbionts) specimens at the end of the 6-
245 week period.

246

247 *3.2 Barium incorporation*

248 Calcite Ba/Ca increases linearly with seawater Ba/Ca for both species (Figure 2; Table 2).
249 ANOVA performed on the individual data points combined with regression analyses reveals a
250 significant increase of Ba/Ca_{cc} with Ba/Ca_{sw} for both species (Table 3). Calculated regression

251 slopes result in a D_{Ba} of 0.326 (± 0.005) for *A. lessonii* and 0.777 (± 0.007) for *H. depressa*
252 (Figure 3, solid lines). Regression lines are forced through zero as it seems reasonable to assume
253 that no Ba is incorporated into calcite when the Ba concentration in the seawater is zero.
254 Without this forcing, regression slopes would be $Ba/Ca_{cc} = 0.34 * Ba/C_{asw} - 1.1$ for *A. lessonii*
255 and $Ba/Ca_{cc} = 0.92 * Ba/C_{asw} - 10$ for *H. depressa*. The resulting partition coefficients
256 ($(Ba/Ca_{cc}) / (Ba/C_{asw})$) are constant and significantly different between the species (ANOVA)
257 (~ 0.3 for *A. lessonii* and ~ 0.8 for *H. depressa*) over the range of seawater Ba/Ca studied here.
258 The regression line for Ba/Ca_{cc} as a function of Ba/C_{asw} for *A. lessonii* corresponds well with
259 that reported for a number of different low Mg species (Lea and Boyle, 1989).
260 The aquarium-derived specimens 'aquarium samples' had an diameter ranging from 550 to
261 1180 μm (with an average of 975 μm) for *A. lessonii* and from 1380 to 2340 μm (average: 1936
262 μm) for *H. depressa*. They had an average Ba/Ca of 15.4 (± 2.3 SD) $\mu mol/mol$ for *A. lessonii*
263 and 35.7 (± 14 SD) $\mu mol/mol$ for *H. depressa*. In combination with the measured aquarium's
264 seawater Ba/Ca of 35.7 (± 3.9 SD) $\mu mol/mol$, the partition coefficients for Ba vary between 0.43
265 and 1.0 for *A. lessonii* and *H. depressa*, respectively. The aquarium derived data is consistent
266 with the controlled growth derived data, but it was not used in the regression analysis (Figure
267 2) since the conditions (e.g. carbonate chemistry) under which the specimens from the aquarium
268 were grown, were not determined as precisely and accurately as in our culturing experiment.
269 Including these data in the linear regression (Figure 2) would change the sensitivity from 0.78
270 to 0.77 for *H. depressa* and from 0.33 to 0.32 for *A. lessonii*.

271

272 3.3 Intrachamber variability in Ba/Ca

273 From both species, 10 specimens were used to quantify the relation between ontogeny (i.e. size-
274 dependent) and Ba incorporation into foraminiferal calcite. For this purpose, the final 6-7
275 chambers of these individuals were ablated (Figure 3). With the selected spot diameter (80 μm),

276 ablation of a small amount of material of adjacent chambers could not always be avoided. Some
277 chamber walls, particularly of the youngest (i.e. built latest) chambers, were too thin for reliable
278 measurements and were excluded from further consideration.

279 Since these specimens were cultured at different Ba/Ca_{sw}, the inter-chamber variability is
280 expressed as the difference of a single-chamber Ba/Ca and the individual's average Ba/Ca.
281 Positive single-chamber values indicate higher than average values, whereas negative values
282 indicate single-chamber Ba/Ca below that individual's average Ba/Ca (Figure 3).

283

284 In *H. depressa*, Ba/Ca_{cc} increases significantly with subsequently new chambers added (Figure
285 3). Regression analysis reveals an average increase of 1.43 μmol/mol Ba/Ca_{cc} with every
286 chamber added (Table 4). Ba/Ca_{cc} appears to decrease with chamber position in *A. lessonii*,
287 although the ANOVA p-value shows that this is statistically not significant. Still, removing one
288 single outlier already results in a p-value lower than 0.01, indicating that the current data set
289 does not allow rejecting the presence of a trend for *A. lessonii*.

290

291 3.4 Relation between incorporation of barium and magnesium

292 Combining data from all five treatments, average Mg/Ca of *A. lessonii* was 64 mmol/mol, with
293 a relative standard deviation of 47%. Within treatments, the variability in Mg/Ca is considerably
294 lower (between 27 and 37%). Average Mg/Ca in *H. depressa* was 152 mmol/mol, with a
295 standard deviation of 25 mmol/mol (16%). Within treatments, the relative standard deviation
296 ranged from 4.1% (treatment E) to 17% (treatment D). The species-specific single-chamber
297 Mg/Ca and Ba/Ca combined for all treatments are positively and significantly related (Figure
298 4). For *A. lessonii*, $Mg/Ca = 3.1 * Ba/Ca - 3.6$ (t-value = 12.2, p < 0.01 for the slope of the
299 regression) and for *H. depressa*, $Mg/Ca = 1.1 * Ba/Ca + 92$ (t-value = 14.8, p < 0.01 for the slope).
300 The slopes of these two regressions (3.1 and 1.1) are significantly different: this is calculated

301 by $z = (a_{Heterostegina} - a_{Amphistegina}) / \sqrt{(SE_{a,Heterostegina}^2 + SE_{a,Heterostegina}^2)}$, where a is the value for the
302 regression's slope and SE_a is the slope's associated standard error. For the slopes of the Mg/Ca-
303 Ba/Ca regressions for *Amphistegina* and *Heterostegina*, the resulting z-score is higher than >7 ,
304 indicating that the two slopes are significantly different.

305 When comparing the single-chamber D_{Ba} with D_{Mg} , of all data combined, the partition
306 coefficient for Mg is over 30 times lower than that of for Ba (Figure 4). Over the range in
307 Ba/ Ca_{sw} studied here, the relation between D_{Ba} and D_{Mg} is linear within both species. For *A.*
308 *lessonii*, $D_{Mg} = 40 * D_{Ba} - 2.0$ (t-value = 7.3, $p < 0.01$ for the slope of the regression) and for *H.*
309 *depressa*, $D_{Mg} = 29 * D_{Ba} + 3.8$ (t-value = 6.5, $p < 0.01$ for the slope). The slopes of these two
310 regressions (40 and 29) are not significantly different (z-score 1.6). When combining the data
311 from both species, the regression equals: $D_{Mg} = 34 * D_{Ba} + 0.073$ (t-value = 29.9, $p < 0.01$ for the
312 slope).

313

314 **4 Discussion**

315 *4.1 Test diameter increase*

316 The range of Ba concentrations used in the experiments did not influence the increase in shell
317 diameter of either foraminiferal species (Figure 1). Compared to *H. depressa*, increases in shell
318 diameter (which is proportional to the chamber addition rate) for *A. lessonii* were slightly more
319 variable. To prevent barite precipitation it was necessary to reduce the sulphate concentration
320 below that typically measured in natural seawater. Sulphate concentrations between 0.1 and 1
321 mmol/L do not affect inorganic calcite growth (Reddy and Nancollas, 1976), but a decrease in
322 growth rates of approximately 30% was observed in coccolithophores growing in artificial
323 seawater with a sulphate concentration 10% that of natural seawater (Langer et al., 2009).
324 Although coccolithophores and foraminifera may respond differently to lowered sulphate
325 concentrations, this reduction could have hampered growth of the specimens in our culturing

326 experiment. Chamber addition rates of *A. lessonii* in a culture set-up with a sulphate
327 concentrations similar to that of natural seawater (Mewes et al., 2014) were approximately 20%
328 higher than chamber addition rates observed in our experiments. Since these experiments were
329 not performed simultaneously using specimens from the same batch, it is not straight forward
330 to compare absolute rates and therefore the 20% difference cannot unambiguously be attributed
331 to sulphate concentration (Hoppe et al. 2011). Unfortunately no data exist on the effect of
332 reduced sulphate concentrations on the uptake of trace elements in foraminiferal calcite.
333 However Langer et al. (2009) demonstrated that sulphate limitation had no discernible effect
334 on Ba incorporation in coccolithophore calcite.

335

336 *4.2 Barium incorporation*

337 The variability in Ba/Ca between individual ablation craters is considerable, but the average
338 foraminiferal Ba/Ca shows a consistent relation with seawater Ba/Ca. This implies that the
339 observed variability is a reflection of the inhomogeneous distribution in the test and hence
340 filtered out when averaging. This is similar to the behavior for Mg and Sr (Sadekov et al., 2008;
341 Wit et al., 2012; De Nooijer et al., 2014a) and underscores the power of single-chamber
342 analyses. If present, inhomogeneity in test wall Ba/Ca in combination with different cross
343 section sampled during the ablation potentially account for the observed variability. This would
344 imply that although large differences are observed within a test wall, the average still reliably
345 reflects sea water concentration (this paper) and for Mg, still reflects seawater temperature
346 (Hathorne et al., 2009). Comparing within-specimen and between-specimen variability, De
347 Nooijer et al. (2014a) showed that within specimen variability does not account for all of the
348 observed variability in Mg/Ca in *Ammonia tepida*. This seems to be similar for Ba/Ca (compare
349 Figure 4 in this paper with Figure 5 from De Nooijer et al., 2014a), which would mean that at
350 least 20 chambers need to be analyzed to reach a 5% relative precision (De Nooijer et al.,

351 2014a). This is not limited by the analytical precision, but rather due to inherent biological inter-
352 chamber and inter-specimen variability. To reduce ontogenetic variability (in e.g.
353 paleoceanographic applications where complete specimens are measured), a narrow size
354 fraction should be analyzed.

355 Incorporation of Ba in *H. depressa* shows a partitioning which is about 2.5 times higher than in
356 *A. lessonii*. Such a large offset of D_{Ba} between benthic species fits previously reported
357 (differences in) partition coefficients for barium. Lea and Boyle (1989) found $D_{Ba} = 0.37 \pm 0.06$
358 for *Cibicoides wuellerstorfi*, *Cibicoides kullenbergi* and *Uvigerina* spp. for a series of core
359 tops, comparable to the partition coefficient reported here for *A. lessonii* (0.33 ± 0.022 ; Figure
360 2). In contrast, partition coefficients for Ba in planktonic foraminifera are roughly only twice
361 as low as these benthic foraminiferal partitioning coefficients (0.14-0.19; Hönisch et al., 2011;
362 Lea and Boyle, 1991; Lea and Spero, 1992). Although temperature, pH, salinity and pressure
363 were initially proposed as potential explanation for the offset between planktonic and benthic
364 D_{Ba} (Lea and Boyle, 1991; Lea and Spero, 1992), studies by Lea and Spero (1994) and Hönisch
365 et al. (2011) showed no significant impact of temperature, pH and salinity on Ba incorporation
366 into planktonic foraminiferal calcite. This would leave hydrostatic pressure to explain the
367 difference between benthic and planktonic species. Van Dijk et al. (2017) on the other hand,
368 showed that in a number of larger benthic foraminifera, Ba/Ca is positively influenced by pCO_2 .
369 Our observations show, however, that the observed differences in D_{Ba} between *H. depressa* and
370 *A. lessonii* and also the offset with the planktonic species are inherent to these species. A small
371 impact of environmental parameters other than seawater Ba/Ca may account for the slightly
372 higher D_{Ba} in the foraminifera taken from the aquarium compared to the cultured ones (Figure
373 2). The overall differences in partitioning seem to coincide with different taxonomic groups,
374 which may indicate that foraminifera may differ in their controls on transporting ions from
375 seawater to the site of calcification. For example, the contribution of transmembrane transport

376 versus that of seawater transport (i.e. leakage; Nehrke et al., 2013 or vacuolization; Erez, 2003)
377 may vary between species and thereby account for differences in Mg/Ca, Ba/Ca, etc. (Nehrke
378 et al., 2013).

379

380 4.3 Inter-chamber variability of Ba/Ca_{cc}

381 In both species cultured here, Ba/Ca_{cc} decreases significantly from largest (i.e. built latest in
382 life) towards the smaller chambers (Figure 3). Observed trends were not significantly different
383 between *A. lessonii* and *H. depressa*, suggesting that Ba/Ca_{cc} decreases at the same rate with
384 size, despite the overall difference in Ba/Ca_{cc} (Figure 3). Since we always analyzed chambers
385 at the same position (F-1 for *A. lessonii* and F-2 for *H. depressa*) and since the final size of the
386 cultured specimens was similar between treatments (Figure 1), ontogenetic trends in Ba/Ca do
387 not influence the trends in Ba/Ca between treatments (Figure 2). Several other studies showed
388 that element/Ca ratios can vary with chamber position. Raitzsch et al. (2011), for example,
389 reported increasing B/Ca and decreasing Mg/Ca towards younger chambers in the benthic
390 *Planulina wuellerstorfi*. Such patterns may be related to changes in the surface-to-volume ratio
391 or relative changes in “vital effects” as foraminifera grow larger. For example, pH reduction in
392 the foraminiferal microenvironment is related to the specimen’s size (Glas et al., 2012) and may
393 thereby affect the chemical speciation of minor and trace element, which in turn, may determine
394 their uptake rates. Hönisch et al. (2011), however, showed that seawater pH has no noticeable
395 effect on Ba incorporation in planktonic foraminiferal calcite, rendering changes in the pH of
396 the foraminiferal microenvironment an unlikely explanation to account for the observed
397 chamber-to-chamber variability in Ba/Ca. Alternatively, changes in the metabolic rate, the
398 instantaneous calcification rate, or a different partitioning between the impacts of the life
399 processes may lead to the observed ontogenetic trend.

400 Bentov and Erez (2006) argued that decreasing Mg/Ca with foraminifera test size could be
401 explained by relatively high Mg-concentrations at or near the primary organic sheet (POS),
402 which is the organic matrix on which the first layer of calcite precipitates during the formation
403 of a new chamber. With the formation of a new chamber, a low-Mg calcite layer is deposited
404 over all existing chambers, so that the high-Mg phase is being 'diluted' as more layers are
405 deposited (Bentov and Erez, 2006). Future studies may indicate whether Ba/Ca is also
406 heterogeneously distributed within chamber walls, by for example, being enriched close to the
407 POS (Kunioka et al., 2006). If this is the case, lamellar calcification mode may also result in
408 changing Ba/Ca with chamber position.

409

410 *4.4 Coupled incorporation of barium and magnesium*

411 If incorporation of Ba and Mg (and Na, Sr and B) are physically linked during
412 biomineralization, inter-species differences in composition may likely be correlated across the
413 various elements. The correlation between Mg/Ca and Ba/Ca within and between species
414 (Figure 4) suggests that these two elements are simultaneously affected during their
415 incorporation. The relationship between Mg/Ca and Ba/Ca is different between the two species,
416 which may be (partly) caused by the variability in seawater chemistry between treatments (i.e.
417 seawater Ba/Ca and Mg/Ca; Table 1). Alternatively, incorporation of Mg in *H. depressa* may
418 be close to the maximum concentration of Mg which can be incorporated into a calcite crystal
419 lattice at ambient conditions (Morse et al., 2007). This may result in an overall asymptotic
420 relationship between Mg/Ca and Ba/Ca as Mg/Ca approaches ~200 mmol/mol (Figure 4).

421 When correcting for the different seawater Ba/Ca and Mg/Ca between treatments, incorporated
422 Ba and Mg correlate similarly within, as well as, between the two species studied here (Figure
423 4). This suggests that these elements are coupled during biomineralization itself and that the
424 ratio of Ba and Mg in seawater is preserved during calcification by these species of

425 foraminifera. When comparing the relation between Ba/Ca and Mg/Ca from other benthic
426 species (e.g. Lea and Boyle, 1989; figure 2; more refs), the coupling between Ba- and Mg-
427 incorporation is likely similar across a wide range of benthic foraminiferal species.

428

429 *4.5 Biomineralization and element incorporation*

430 Foraminiferal biomineralization determines incorporation of many elements and fractionation
431 of many isotopes during the production of new chambers as indicated by overall large
432 compositional differences between inorganically precipitated and foraminiferal calcite (Erez,
433 2003; Bentov and Erez, 2006; Nehrke et al., 2013; De Nooijer et al., 2014b). For example,
434 Mg/Ca ratios in many species are orders of magnitude lower than what is expected from
435 inorganic precipitation experiments. Additionally, Mg/Ca varies considerably between
436 foraminiferal species and especially between species known to have different calcification
437 strategies (Bentov and Erez, 2006; Toyofuku et al., 2011; Wit et al., 2012; De Nooijer et al.,
438 2009; 2014b). Other elements such as Sr (e.g. Elderfield et al., 2000) and B/Ca (e.g. Allen et
439 al., 2012) also vary significantly between species. Generally, concentrations for these elements
440 correlate within taxa and hence species incorporating relatively much Mg, also have high (for
441 example) Sr/Ca, B/Ca and Na/Ca. Miliolids and many 'Large Benthic Foraminifera' (LBF)
442 produce calcite with Mg/Ca up to 100-150 mmol/mol (Toyofuku et al., 2000; Dueñas-
443 Bohórquez et al., 2011; Sadekov et al., 2014; Evans et al., 2015), while most planktonic and
444 symbiont-barren benthic foraminifera produce test calcite with Mg/Ca values ranging from 1-
445 10 mmol/mol (e.g. Nürnberg et al., 1996; Elderfield et al., 2002; Lear et al., 2010; Wit et al.,
446 2012; De Nooijer et al., 2014b). The same distinction is observed for B/Ca (compare e.g. Allen
447 et al., 2012 and Kazcmarek et al., 2015), Li/Ca (Lear et al., 2010 versus Evans et al., 2015),
448 Na/Ca (Wit et al., 2013 versus Evans et al., 2015) and Sr/Ca (e.g. Dueñas-Bohórquez et al.,
449 2011). The correlation between relatively high (for example) Mg/Ca, Sr/Ca and B/Ca

450 corresponds to the observed trends in the data presented here for Ba/Ca and Mg/Ca in *H.*
451 *depressa* and *A. lessonii* (Figure 4). The Mg/Ca in the former species is approximately 2.5 times
452 that of the latter, which is similar to the difference observed in Ba/Ca ratios between these
453 species and implies that Ba changes in concert with Mg, which is consistent with the single-
454 chamber correlation between Mg/Ca and Ba/Ca (Figure 4). Such a change could potentially be
455 caused inorganically by differences in Mg opening up the crystal lattice in such a way that it
456 can accommodate more or less Ba. Such a mechanism is described for Mg and Sr (e.g. Morse
457 and Bender, 1990; Mucci and Morse, 1983; Mewes et al., 2015; Langer et al., 2016) and may
458 also apply to Ba incorporation and the influence of Mg ions that increase stress in the calcite
459 crystal lattice. Unless the strain of incorporated Mg ions does not increase linearly with its
460 concentration, the covariance between Mg and in this case Ba may well be interrelated during
461 an earlier stage of the biomineralization process, e.g. during their transport from the surrounding
462 seawater into the site of calcification (Erez, 2003; De Nooijer et al., 2014b).

463 Interestingly, the partitioning of different elements is not the same between taxa. For example,
464 Sr/Ca in LBFs is approximately twice as high (Dueñas-Bohorquez et al., 2011; Evans et al.,
465 2015) as in planktonic species (Elderfield et al., 2002; Dueñas-Bohórquez et al., 2009; Hendry
466 et al., 2009), whereas the ratio between the D_{Mg} of these groups is between 10 and 100 (see
467 above). Comparing the offset of D between groups as a function of D itself shows an
468 approximate logarithmic correlation (Figure 5). The distinction between the two groups on basis
469 of their element signature coincides with known differences in biomineralization controls.

470 Element controls in low-Mg species are thought to be determined by (highly) selective trans-
471 membrane ion transporters, (limited) leakage of seawater into the site of calcification and/or
472 selective Mg^{2+} -removal (Nehrke et al., 2013; De Nooijer et al., 2014b; Toyofuku et al., 2017).

473 Miliolid foraminifera belong to the high-Mg foraminiferal group and are known to secrete their
474 calcite within vesicles that are hypothesized to contain seawater, which may be modified after

475 endocytosis (Hemleben et al., 1986; Ter Kuile and Erez, 1991; De Nooijer et al., 2009). These
476 intracellular vesicles may therefore contain relatively high concentrations of Mg^{2+} , Ba^{2+} and
477 other ions present in seawater, although so far mainly Sr/Ca and Mg/Ca of Miliolid foraminifera
478 have been published (supplementary information). The biomineralization of non-Miliolid,
479 intermediate- and high-Mg benthic foraminifera may employ characteristics of both these types
480 of calcification and therefore incorporate moderately to high concentrations of elements (cf
481 Segev and Erez, 2006).

482

483 **5 Conclusions**

484 Results from this study indicate that differences in D_{Ba} between species of foraminifera can be
485 relatively large. This implies that species-specific Ba partition coefficients need to be applied
486 to reconstruct past Ba/Ca_{sw} and/or salinity (Lea and Boyle, 1989; Weldeab et al., 2007;
487 Hoffmann et al., 2014; Evans et al., 2015). Moreover, our results underscore the necessity to
488 account for size-related effects on Ba/Ca_{cc} . This effect may bias obtained Ba/Ca_{cc} particularly
489 when using single chamber measurements. When determining Ba/Ca_{cc} by dissolution of whole
490 shells, the contribution of smaller chambers (with lower Ba/Ca_{cc}) is relatively small compared
491 to a specimen's overall Ba/Ca and thus does not affect average values. Our results also show
492 that within species as well as between species, single-chambered Mg/Ca and Ba/Ca are linearly
493 correlated. The difference in Ba/Ca between the two species studied here fits with previously
494 observed variability in element/Ca ratios between foraminifera taxa and likely reflects
495 differences in their biomineralization mechanisms.

496

497 **References**

498 Allen, K.A., Hönisch, B., Eggins, S.M., Yu, J., Spero, H.J., Elderfield, H., 2011. Controls on
499 Boron incorporation in cultured tests of the planktic foraminifer *Orbulina universa*.
500 Earth Planet. Sci. Lett. 309, 291-301.

501 Allen, K.A., Hönisch, B., Eggins, S.M., Rosenthal, Y., 2012. Environmental controls on B/Ca
502 in calcite tests of the tropical planktic foraminifer species *Globigerinoides ruber* and
503 *Globigerinoides sacculifer*. Earth Planet. Sci. Lett. 351-352, 270-280.

504 Babila, T.L., Rosenthal, Y., Conte, M.H., 2014. Evaluation of the biogeochemical controls on
505 B/Ca of *Globigerinoides ruber* from the Ocean Flux Program, Bermuda. Earth Planet.
506 Sci. Lett. 404, 67-76.

507 Bahr, A., Schönfeld, J., Hoffmann, J., Voigt, S., Aurahs, R., Kucera, M., Slögel, S., Jentzen,
508 A., Gerdes, A., 2013. Comparison of Ba/Ca and $\delta^{18}\text{O}_{\text{water}}$ as freshwater proxies: A
509 multi-species core-top study on planktonic foraminifera from the vicinity of the
510 Orinoco River mouth. Earth Planet. Sci. Lett. 383, 45-57.

511 Bentov, S., Erez, J., 2006. Impact of biomineralization processes on the Mg content of
512 foraminiferal shells: A biological perspective. *Geochem. Geophys. Geosyst.* 7,
513 Q01P08.

514 Bian, N., Martin, P.A., 2010. Investigating the fidelity of Mg/Ca and other element data from
515 reductively cleaned planktonic foraminifera. *Paleoceanography* 25, PA2215.

516 Boyle, E.A., 1981. Cadmium, zinc, copper and barium in foraminifera tests. Earth Planet. Sci.
517 Lett. 53, 11-35.

518 Bradshaw, A.L., Brewer, P.G., Shafer, D.K., Williams, R.T., 1981. Measurements of total
519 carbon dioxide and alkalinity by potentiometric titration in the GEOSECS program.
520 Earth Planet. Sci. Lett. 55, 99-115.

521 Broecker W.S., Peng T.-H., 1982. *Tracers in the Sea*, Eldigo Press, Lamont-Doherty
522 Geological Observatory, Palisades, New York, USA, pp. 690.

- 523 Bryan, S.P., Marchitto, T.M., 2008. Mg/Ca-temperature proxy in benthic foraminifera: New
524 calibrations from the Florida Straits and a hypothesis regarding Mg/Li.
525 *Paleoceanography* 23, PA2220.
- 526 Chan, L.H., Drummond, D., Edmond, J.M., Grant, B., 1977. On the barium data from the
527 Atlantic GEOSECS expedition. *Deep-Sea Res.* 24, 613-649.
- 528 Dawber, C.F., Tripathi, A., 2012. Relationships between bottom water carbonate saturation and
529 element/Ca ratios in coretop samples of the benthic foraminifera *Oridorsalis*
530 *umbonatus*. *Biogeosciences* 9, 3029-3045.
- 531 De Nooijer, L.J., Toyofuku, T., Kitazato, H., 2009. Foraminifera promote calcification by
532 elevating their intracellular pH. *Proc. Natl. Acad. Sci. USA* 106, 15374-15378.
- 533 De Nooijer, L.J., Hathorne, E.C., Reichart, G.J., Langer, G., Bijma, J., 2014a. Variability in
534 calcitic Mg/Ca and Sr/Ca ratios in clones of the benthic foraminifer *Ammonia tepida*.
535 *Marine Micropaleontology* 107, 33-43.
- 536 De Nooijer, L.J., Spero, H.J., Erez, J., Bijma, J., Reichart, G.J., 2014b. Biomineralization in
537 perforate foraminifera. *Earth-Sci. Rev.* 135, 48-58.
- 538 Dickson, A.G., Millero, F.J., 1987. A comparison of the equilibrium constants for dissociation
539 constants of carbonic acid in seawater media. *Deep Sea Res.* 34, 1733-1743.
- 540 Dueñas-Bohórquez, A., Da Rocha, R., Kuroyanagi, A., Bijma, J., Reichart, G.J., 2009. Effect
541 of salinity and seawater calcite saturation state on Mg and Sr incorporation in cultured
542 planktonic foraminifera. *Marine Micropaleontology* 73, 178-189.
- 543 Dueñas-Bohórquez, A., Raitzsch, M., De Nooijer, L.J., Reichart, G.J., 2011. Independent
544 impacts of calcium and carbonate ion concentration on Mg and Sr incorporation in
545 cultured benthic foraminifera. *Marine Micropaleontology* 81, 122-130.

546 Eggins, S., De Deckker, P., Marshall, J., 2003. Mg/Ca variation in planktonic foraminifera tests:
547 implications for reconstructing palaeo-seawater temperature and habitat migration.
548 Earth Planet. Sci. Lett. 212, 291-306.

549 Elderfield, H., Cooper, M., Ganssen, G., 2000. Sr/Ca in multiple species of planktonic
550 foraminifera: Implications for reconstructions of seawater Sr/Ca. Geochem. Geophys.
551 Geosyst. 1, GC000031.

552 Elderfield, H., Vautravers, M., Cooper, M., 2002. The relationship between shell size and
553 Mg/Ca, Sr/Ca, $\delta^{18}\text{O}$, and $\delta^{13}\text{C}$ of species of planktonic foraminifera. Geochem.
554 Geophys. Geosyst. 3, GC000194.

555 Elderfield, H., Yu, J., Anand, P., Kiefer, T., Nyland, B., 2006. Calibrations for benthic
556 foraminiferal Mg/Ca paleothermometry and the carbonate ion hypothesis. Earth
557 Planet. Sci. Lett. 250, 633-649.

558 Erez, J., 2003. The source of ions for biomineralization in foraminifera and their implications
559 for paleoceanographic proxies. Rev. Mineral. Geochem. 54, 115-149.

560 Evans, D., Erez, J., Oron, S., Müller, W., 2015. Mg/Ca-temperature and seawater-test chemistry
561 relationships in the shallow-dwelling large benthic foraminifera *Operculina*
562 *ammonoides*. Geochim. Cosmochim. Acta 148, 325-342.

563 Foster, G.L., 2008. Seawater pH, $p\text{CO}_2$ and $[\text{CO}_3^{2-}]$ variations in the Caribbean Sea over the
564 last 130 kyr: A boron isotope and B/Ca study of planktonic foraminifera. Earth and
565 Planetary Science Letters 271, 254-266.

566 Glas, M.S., Langer, G., Keul, N., 2012. Calcification acidifies the microenvironment of a
567 benthic foraminifer (*Ammonia* sp.). J. Exp. Mar. Biol. Ecol. 424-425, 53-58.

568 Gran, G., 1952. Determination of the equivalence point in potentiometric titrations-- Part II.
569 The Analyst 77, 661-671.

570 Guay, C.K., Falkner, K.K., 1997. Barium as a tracer of Arctic halocline and river waters,
571 Deep Sea Res. Part II 44, 1543– 1569.

572 Guay, C.K., Falkner, K.K., 1998. A survey of dissolved barium in the estuaries of major
573 Arctic rivers and adjacent seas. Cont. Shelf Res. 18, 859– 882.

574 Guillong, M., Meier, D.L., Allan, M.M., Heinrich, C.A., Yardley, B.W.D., 2008. SILLS: A
575 MATLAB-based program for the reduction of laser ablation ICP-MS data of
576 homogeneous materials and inclusions. Mineralogical Association of Canada Short
577 Course 40, 328-333.

578 Hall, J.M., Chan, L.-H., 2004a. Li/Ca in multiple species of benthic and planktonic
579 foraminifera: Thermocline, latitudinal, and glacial-interglacial variation. Geochim.
580 Cosmochim. Acta 68, 529-545.

581 Hall, J.M., Chan, L.-H., 2004b. Ba/Ca in *Neogloboquadrina pachyderma* as an indicator of
582 deglacial meltwater discharge into the western Arctic Ocean. Paleoceanography 19,
583 PA000910.

584 Hanor, J.S., Chan, L.-H., 1977. Non-conservative behavior of barium during mixing of
585 Mississippi River and Gulf of Mexico waters. Earth Planet. Sci. Lett. 37, 242–250.

586 Hathorne, E.C., James, R.H., Savage, P., Alard, O., 2008. Physical and chemical characteristics
587 of particles produced by laser ablation of biogenic calcium carbonate. J. Anal. Atom.
588 Spectrom. 23, 240-243.

589 Hathorne, E.C., James, R.H., Lampitt, R.S., 2009. Environmental versus biomineralization
590 controls on the intratest variation in the trace element composition of the planktonic
591 foraminifera *G. inflata* and *G. scitula*. Paleoceanography 24, PA001742.

592 Hemleben, C., Anderson, O.R., Berthold, W., Spindler, M., 1986. Calcification and chamber
593 formation in foraminifera - an overview. pp 237-249. In: Biomineralization in lower

594 plants and animals, Leadbeater, B.S.C. and Riding, R. (eds) The Systematics Society,
595 London.

596 Hendry, K.R., Rickaby, R.E.M., Meredith, M.P., Elderfield, H., 2009. Controls on stable
597 isotope and trace metal uptake in *Neogloboquadrina pachyderma* (sinistral) from an
598 Antarctic sea-ice environment. *Earth Planet. Sci. Lett.* 278, 67-77.

599 Hatch, M.B.A., Schellenberg, S.A., Carter, M.L., 2013. Ba/Ca variations in the modern
600 intertidal bean clam *Donax gouldii*: An upwelling proxy? *Palaeogeogr. Palaeoclim.*
601 *Palaeoecol.* 373, 98-107.

602 Hoffmann, J., Bahr, A., Voigt, S., Schönfeld, J., Nürnberg, D., Rethemeyer, J., 2014.
603 Disentangling abrupt deglacial hydrological changes in northern South America:
604 Insolation versus oceanic forcing. *Geology* 42, 579-582.

605 Hönisch, B., Allen, K.A., Russell, A.D., Eggins, S.M., Bijma, J., Spero H.J., Lea, D.W., Yu, J.,
606 2011. Planktic foraminifers as recorders of seawater Ba/Ca. *Marine*
607 *Micropaleontology* 79, 52-57.

608 Hoppe, C.J.M., Langer, G., Rost, B., 2011. *Emiliana huxleyi* shows identical responses to
609 elevated pCO₂ in TA and DIC manipulations. *J. Exp. Mar. Biol. Ecol.* 406, 54–62.

610 Jochum, K.P., Weis, U., Stoll, B., Kuzmin, D., Yang, Q., Raczek, I., Jacob, D.E., Stracke, A.,
611 Birbaum, K., Frick, D.A., Günther, D.,ENZWEILER, J., 2011. Determination of
612 reference values for NIST SRM 610-617 glasses following ISO guidelines. *Geostand.*
613 *Geoanal. Res.* 35, 397-429.

614 Kaczmarek, K., Langer, G., Nehrke, G., Horn, I., Misra, S., Janse, M., Bijma, J., 2015. Boron
615 incorporation in the foraminifer *Amphistegina lessonii* under a decoupled carbon
616 chemistry. *Biogeosciences* 12, 1753-1763.

617 Kester, D.R., Duedall, I.W., Connors, D.N., 1967. Preparation of artificial seawater. *Limnol.*
618 *Oceanogr.* 12, 176-179.

619 Kunioka, D., Shirai, K., Takahata, N., Sano, Y., Toyofuku, T., Ujiie, Y., 2006.
620 Microdistribution of Mg/Ca, Sr/Ca, and Ba/Ca ratios in *Pulleniatina obliquiloculata*
621 test by using a NanoSIMS: Implication for the vital effect mechanism. *Geochem.*
622 *Geophys. Geosyst.* 7, GC001280.

623 Langer, G., Nehrke, G., Thoms, S., Stoll, H., 2009. Barium partitioning in coccoliths of
624 *Emiliana huxleyi*. *Geochim. Cosmochim. Acta* 73, 2899-2906.

625 Langer G., Sadekov, A., Thoms, S., Keul, N., Nehrke, G., Mewes, A., Greaves, M., Misra, S.,
626 Reichart, G.J., De Nooijer, L.J., Bijma, J., Elderfield, H., 2016. Sr partitioning in the
627 benthic foraminifera *Ammonia aomoriensis* and *Amphistegina lessonii*. *Chemical*
628 *Geology* 440: 306-312.

629 Lea, D.W., 1995. A trace metal perspective on the evolution of Antarctic circumpolar deepwater
630 chemistry. *Paleoceanography* 10, 733-747.

631 Lea, D., Boyle, E., 1989, Barium content of benthic foraminifera controlled by bottom-water
632 composition. *Nature* 338, 751-753.

633 Lea, D.W., Shen, G.T, Boyle, E.A., 1989. Coralline barium records temporal variability in
634 equatorial Pacific upwelling. *Nature* 340, 373-376.

635 Lea, D.W., Boyle, E.A., 1990. A 210,000-year record of barium variability in the deep
636 northwest Atlantic Ocean. *Nature* 347, 269-272.

637 Lea, D.W., Boyle, E.A. 1991. Barium in planktonic foraminifera. *Geochim. Cosmochim. Acta*
638 55, 3321-3331.

639 Lea, D.W., Boyle, E.A., 1993. Determination of carbonate-bound barium in foraminifera and
640 corals by isotope dilution plasma-mass spectrometry. *Chem. Geol.* 103, 73-84.

641 Lea, D.W., Spero, H.J., 1992. Experimental determination of barium uptake in shells of the
642 planktonic foraminifera *Orbulina universa* at 22° C. *Geochim. Cosmochim. Acta* 56,
643 2673-2680.

644 Lea, D.W., Spero, H.J., 1994. Assessing the reliability of paleochemical tracers: Barium uptake
645 in the shells of planktonic foraminifera. *Paleoceanography* 9, 445-452.

646 Lea, D.W., Mashiotta, T.A., Spero, H.J., 1999. Controls on magnesium and strontium uptake
647 in planktonic foraminifera determined by live culturing. *Geochim. Cosmochim. Acta*
648 63, 2369-2379.

649 Lear, C.H., Mawbey, E.M., Rosenthal, Y., 2010. Cenozoic benthic foraminiferal Mg/Ca and
650 Li/Ca records: Toward unlocking temperatures and saturation states.
651 *Paleoceanography* 25, PA001880.

652 Lee, J.J., 2006. Algal symbiosis in larger foraminifera. *Symbiosis* 42, 63-75.

653 Lewis, E., Wallace, D., 1998. Program developed for CO₂ system calculations, p 38.

654 Li, Y.-H., Chan, L.-H., 1979. Desorption of Ba and ²²⁶Ra from river-borne sediments in the
655 Hudson Estuary. *Earth Planet. Sci. Lett.* 37: 242-250.

656 Marr, J.P., Carter, L., Bostock, H.C., Bolton, A., Smith, E., 2013. Southwest Pacific Ocean
657 response to a warming world: Using Mg/Ca, Zn/Ca, and Mn/Ca in foraminifera to
658 track surface ocean water masses during the last deglaciation. *Paleoceanography* 28,
659 347-362.

660 Marriott, C.S., Henderson, G.M., Crompton, R., Staubwasser, M., Shaw, S., 2004. Effect of
661 mineralogy, salinity, and temperature on Li/Ca and Li isotope composition of calcium
662 carbonate. *Chemical Geology* 212, 5-15.

663 Mehrbach, C., Culberson, C.H., Hawley, J.E., Pytkowicz, R.N., 1973. Measurement of the
664 apparent dissociation constants of carbonic acid in seawater at atmospheric pressure.
665 *Limnol. Oceanogr.* 18, 897-907.

666 Mewes, A., Langer, G., De Nooijer, L.J., Bijma, J., Reichart, G.J., 2014. Effect of different
667 seawater Mg²⁺ concentrations on calcification in two benthic foraminifers. *Marine*
668 *Micropaleontology* 113, 56-64.

669 Mewes, A., Langer, G., Reichart, G.J., De Nooijer, L.J., Nehrke, G., Bijma, J., 2015. The impact
670 of Mg contents on Sr partitioning in benthic foraminifers. *Chem. Geol.* 412, 92-98.

671 Morse, J.W., Bender, M.L., 1990. Partition coefficients in calcite: Examination of factors
672 influencing the validity of experimental results and their application to natural systems.
673 *Chem. Geol.* 82, 265-277.

674 Morse, J.W., Arvidson, R.S., Lüttge, A., 2007. Calcium carbonate formation and dissolution.
675 *Chem. Rev.* 107: 342-381.

676 Mucci, A., Morse, J.W., 1983. The incorporation of Mg^{2+} and Sr^{2+} into calcite overgrowths:
677 influences of growth rate and solution composition. *Geochim. Cosmochim. Acta* 47,
678 217-233.

679 Nehrke, G., Keul, N., Langer, G., De Nooijer, L.J., Bijma, J., Meibom, A., 2013. A new model
680 for biomineralization and trace-element signatures of foraminifera tests.
681 *Biogeosciences* 10, 6759-6767.

682 Ni, Y., Foster, G.L., Bailey, T., Elliott, T., Schmidt, D.N., Pearson, P., Haley, B., Coath, C.,
683 2007. A core top assessment of proxies for the ocean carbonate system in surface-
684 dwelling foraminifera. *Paleoceanography* 22, PA3212.

685 Ni Flaithearta, S., Reichart, G.J., Jorissen, F.J., Fontanier, C., Rohling, E.J., Thomson, J., De
686 Lange, G., 2010. Reconstructing the seafloor environment during sapropel formation
687 using benthic foraminiferal trace metals, stable isotopes, and sediment composition.
688 *Paleoceanography* 25, PA4225.

689 Nürnberg, D., Bijma, J., Hemleben, C., 1996. Assessing the reliability of magnesium in
690 foraminiferal calcite as a proxy for water mass temperatures. *Geochim. Cosmochim.*
691 *Acta* 80, 803-814.

692 Okai, T., Suzuki, A., Kawahata, H., Terashima, S., Imai, N., 2002. Preparation of a New
693 Geological Survey of Japan Geochemical Reference Material: Coral JCp-1,
694 Geostandards Newsletter 26, 95-99.

695 Pak, D.K., Lea, D.W., Kennett, J.P., 2004. Seasonal and interannual variation in Santa Barbara
696 Basin water temperatures observed in sediment trap foraminiferal Mg/Ca. *Geochem.*
697 *Geophys. Geosyst.* 5, Q12008.

698 Pierrot, D., Lewis, E., Wallace, D.W.R., 2006. MS Excel program developed for CO₂ system
699 calculations. ORNL/CDIAC-105. Carbon dioxide Information Analysis Center, Oak
700 Ridge National Laboratory, US department of Energy, Oak Ridge, Tennessee.

701 Raitzsch, M., Hathorne, E.C., Kuhnert H., Groeneveld, J., Bickert, T., 2011. Modern and late
702 Pleistocene B/Ca ratios of the benthic foraminifer *Planulina wuellerstorfi* determined
703 with laser ablation ICP-MS. *Geology* 39, 1039-1042.

704 Raja, R., Saraswati, P.K., Rogers, K., Iwao, K., 2005. Magnesium and strontium compositions
705 of recent symbiont-bearing benthic foraminifera. *Marine Micropaleontology* 58, 31-
706 44.

707 Reddy, M.M., Nancollas, G.H., 1976. The crystallization of calcium carbonate: IV. The effect
708 of magnesium, strontium and sulfate ions. *J. Crystal Growth* 35, 33-38.

709 Reichart, G.J., Jorissen, F., Anschutz, P., Mason, P.R.D., 2003. Single foraminiferal test
710 chemistry records the marine environment. *Geology* 31, 355-358.

711 Rubin, S.I., King, S.L., Jahnke, R.A., Froelich, P.N., 2003. Benthic barium and alkalinity
712 fluxes: Is Ba an oceanic paleo-alkalinity proxy for glacial atmosphere CO₂? *Geophys.*
713 *Res. Lett.* Vol. 30, 1885.

714 Sadekov, A., Eggins, S.M., De Deckker, P., Kroon, D., 2008. Uncertainties in seawater
715 thermometry deriving from intratest and intertest Mg/Ca variability in *Globigerinoides*
716 *ruber*. *Paleoceanography* 23, PA0014502.

717 Sadekov, A., Bush, F., Kerr, J., Ganeshram, R., Elderfield, H., 2014. Mg/Ca composition of
718 benthic foraminifera *Miliolacea* as a new tool of paleoceanography. *Paleoceanography*
719 29, 990-1001.

720 Segev, E., Erez, J., 2006. Effect of Mg/Ca ratio in seawater on shell composition in shallow
721 benthic foraminifera. *Geochem. Geophys. Geosyst.* 7, GC000969.

722 Ter Kuile B.H., Erez, J., 1991. Carbon budgets for two species of benthonic symbiont-bearing
723 foraminifera. *Biological Bulletin* 180, 489-495.

724 Toyofuku, T., Kitazato, H., Kawahata, H., 2000. Evaluation of Mg/Ca thermometry in
725 foraminifera: Comparison of experimental results and measurements in nature.
726 *Paleoceanography* 15, 456-464.

727 Toyofuku, T., Suzuki, M., Suga, H., Sakai, S., Suzuki, A., Ishikawa, T., De Nooijer, L.J.,
728 Schiebel, R., Kawahata, H., Kitazato, H., 2011. Mg/Ca and $\delta^{18}\text{O}$ in the brackish
729 shallow-water benthic foraminifer *Ammonia 'beccarii'*. *Marine Micropaleontology* 78,
730 113-120.

731 Toyofuku, T., Matsuo, M.Y., De Nooijer, L.J., Nagai, Y., Kawada, S., Fujita, K., Reichart, G.-
732 J., Nomaki, H., Tsuchiya, M., Sakaguchi, H., Kitazato, H., 2017. Proton pumping
733 accompanies calcification in foraminifera. *Nature Communications* 8, 14145.

734 Van Dijk, I., De Nooijer, L.J., Reichart, G.-J., 2017. Trends in element incorporation in hyaline
735 and porcelaneous foraminifera as a function of $p\text{CO}_2$. *Biogeosciences* 14, 497-510.

736 Weldeab, S., Lea, D.W., Schneider, R.R., Andersen, N., 2007. 155,000 years of west African
737 monsoon and ocean thermal evolution. *Science* 316, 1303-1307.

738 Weldeab, S., Lea, D.W., Oberhänsli, H., Schneider, R.R., 2014. Links between southwestern
739 tropical Indian Ocean SST and precipitation over southeastern Africa over the last 17
740 kyr. *Palaeogeogr. Palaeoclimatol. Palaeoecol.* 410, 200-212.

741 Wilson, S. A., Koenig, A. E., Orklid, R., 2008. Development of microanalytical reference
742 material (MACS-3) for LA-ICP-MS analysis of carbonate samples, *Geochimica et*
743 *Cosmochimica Acta Supplement* 72, 1025.

744 Wit, J.C., De Nooijer, L.J., Barras, C., Jorissen, F.J., Reichart, G.J., 2012. A reappraisal of the
745 vital effect in cultured benthic foraminifer *Bulimina marginata* on Mg/Ca values:
746 assessing temperature uncertainty relationships. *Biogeosciences* 9, 3693-3704.

747 Wit, J.C., De Nooijer, L.J., Wolthers, M., Reichart, G.J., 2013. A novel salinity proxy based on
748 Na incorporation into foraminiferal calcite. *Biogeosciences* 10, 6375-6387.

749

750 Yu, J., Day, J., Greaves, M., Elderfield, H., 2005. Determination of multiple element/ calcium
751 ratios in foraminiferal calcite by quadrupole ICP-MS. *Geochemistry, Geophysics,*
752 *Geosystems* 6, Q08P01.

753 Yu, J., Elderfield, H., 2007. Benthic foraminiferal B/Ca ratios reflect deep water carbonate
754 saturation state. *Earth and Planetary Science Letters* 258, 73-86.

755

756 **Tables**

757 *Table 1: measured concentrations of major and minor ions, temperature, salinity and*
 758 *carbonate chemistry in the five culture media (A-E).*

Treatment	A	B	C	D	E
Ba (nmol/kg)	488.5	535.5	611.0	608.4	854.6
Ca (mmol/kg)	9.1	9.5	9.6	9.2	9.3
Ba/Ca _{sw} (mmol/mol)	53.68	56.36	63.64	66.14	91.89
Na (mmol/kg)	402	416	389	383	384
B (mmol/kg)	11	11	12	11	11
K(mmol/kg)	0.40	0.46	0.43	0.43	0.42
Mg (mmol/kg)	55	58	59	53	53
Sr (mmol/kg)	0.11	0.11	0.12	0.11	0.11
Mg/Ca _{sw} (mol/mol)	6.04	6.11	6.15	5.76	5.70
T (°C)	25	25	25	25	25
Salinity	32.4	32.4	32.4	32.4	32.4
TA (µmol/kg)	2445	2450	2662	2437	2429
DIC (µmol/kg)	2244 ± 3	2246 ± 6	2464 ± 7	2236 ± 7	2228 ± 9
Ω _{calcite}	3.9	3.9	4.0	3.9	3.9

759

760 *Table 2. Measured Ba/Ca and Mg/Ca for A. lessonii and H. depressa for each treatment.*

Treatment	A	B	C	D	E
<i>A. lessonii</i>					
n	40	43	17	36	43
Ba/Ca (µmol/mol)	15.8	19.6	18.8	22.9	29.9
SD	3.3	3.6	3.0	4.5	5.5

Mg/Ca (mmol/mol)	37.9	49.2	70.1	89.6	80.4
SD	10	13	19	33	29
<i>H. depressa</i>					
n	26	27	23	25	32
Ba/Ca ($\mu\text{mol/mol}$)	41.1	41.5	46.0	50.8	74.9
SD	6.2	4.3	3.9	5.7	3.9
Mg/Ca (mmol/mol)	150	135	123	168	177
SD	12	11	6	29	7

761

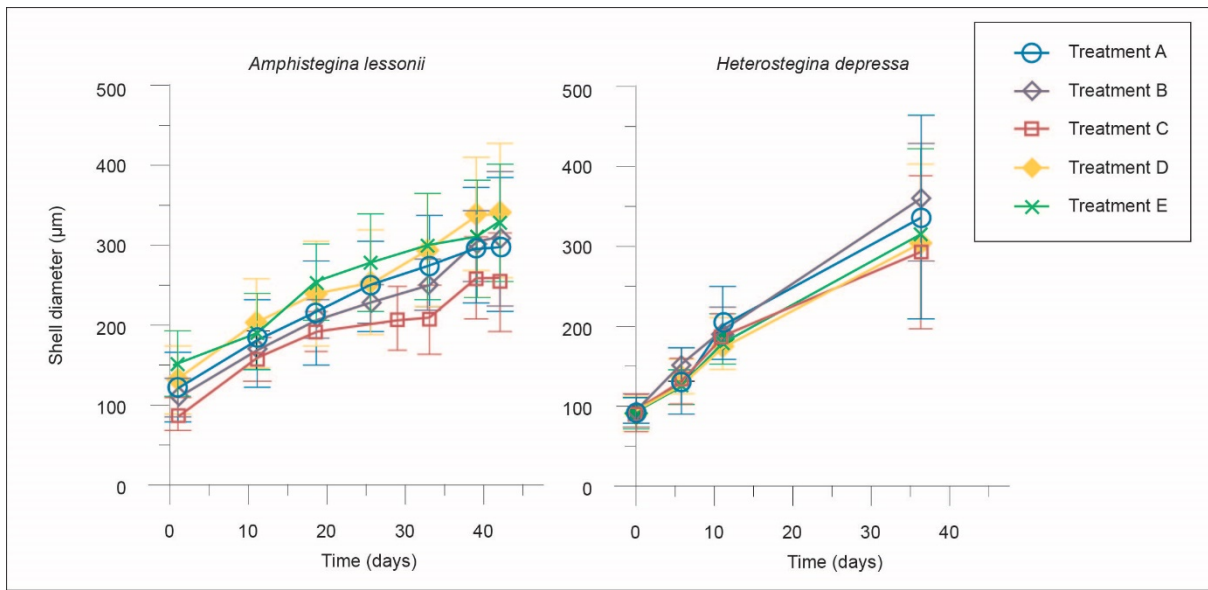
762 *Table 3. Parameters of the regression analysis and ANOVA tests for significance of the*
763 *regression. Both average Ba/Ca_{cc} of each experimental condition (n=5) and all chamber-*
764 *specific Ba/Ca_{cc} (n=133/ 179) were tested versus the Ba/Ca of the 5 treatments.*

			Regression analysis	ANOVA	
Parameter	Species	n	R ²	F-value	p-value
Ba/Ca _{sw} vs Ba/Ca _{cc}	<i>H. depressa</i>	133	0.88	940	<0.01
	<i>A. lessonii</i>	179	0.56	227	<0.01
Ba/Ca _{sw} vs average Ba/Ca _{cc}	<i>H. depressa</i>	5	0.99	247	<0.01
	<i>A. lessonii</i>	5	0.91	32	0.011

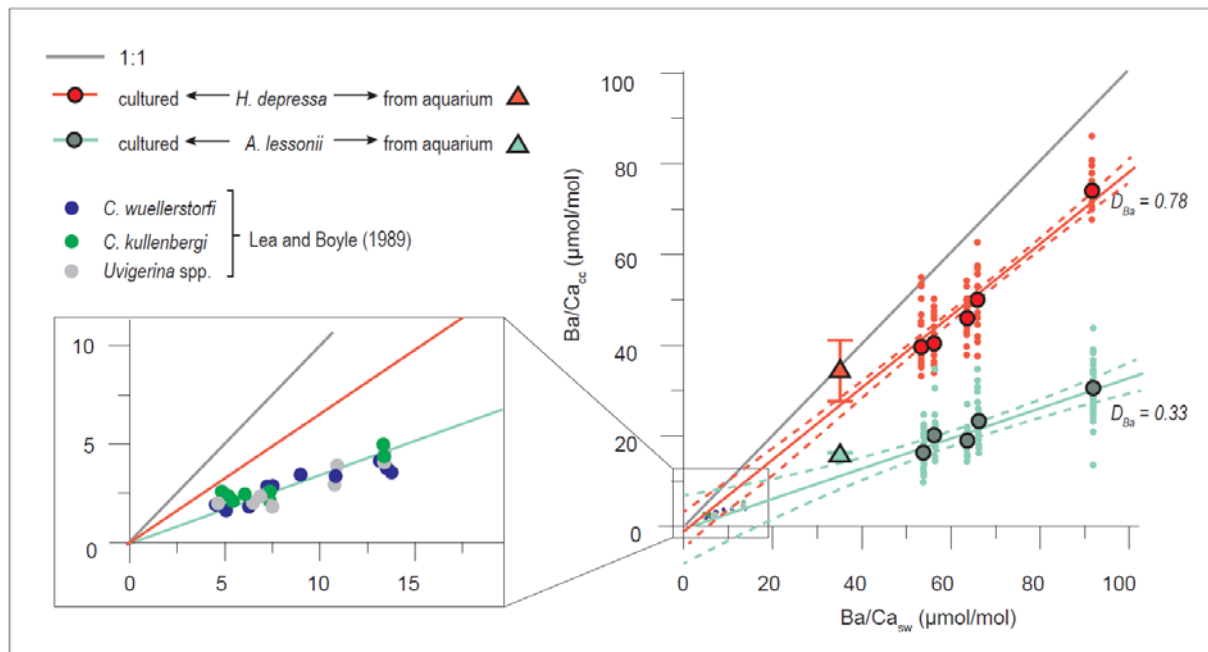
765

766 *Table 4. ANOVA parameters of single-chamber measurements*

ANOVA	Species	F	p
	<i>A. lessonii</i>	2.47	0.06
	<i>A. lessonii</i> (f-1 and f-2)	0.11	0.744
	<i>H. depressa</i>	6.09	< 0.01

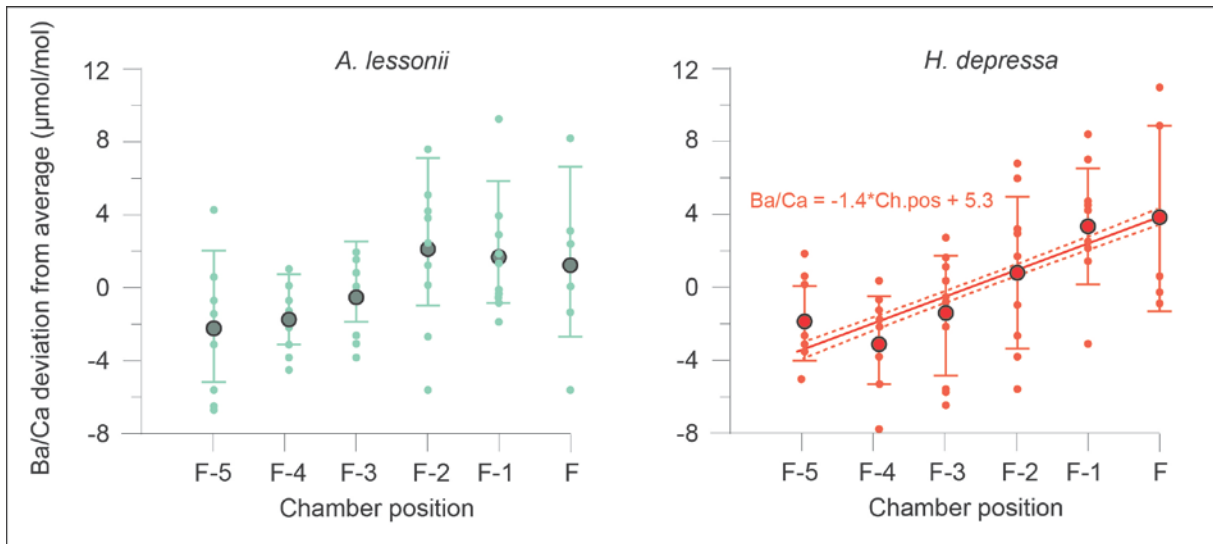


768

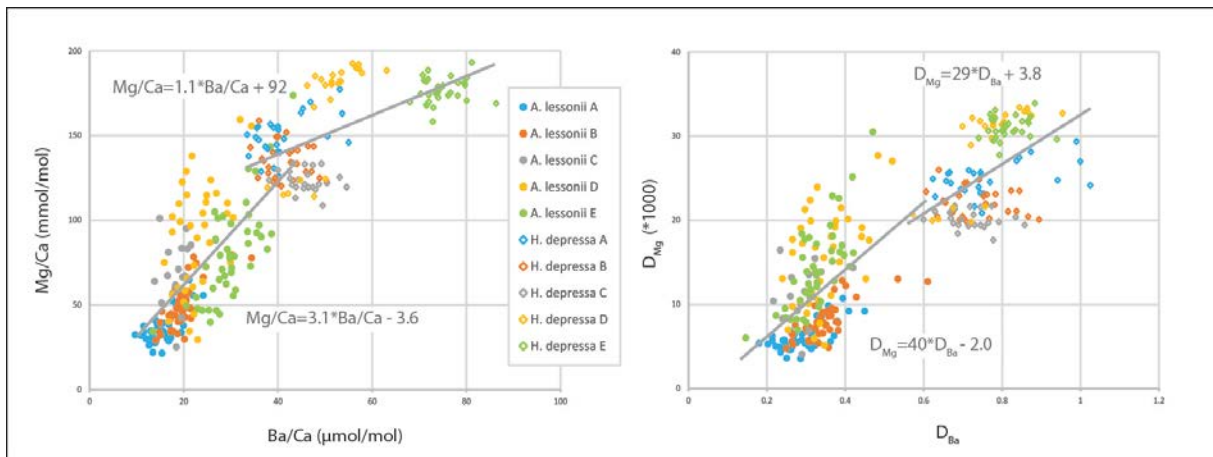


769

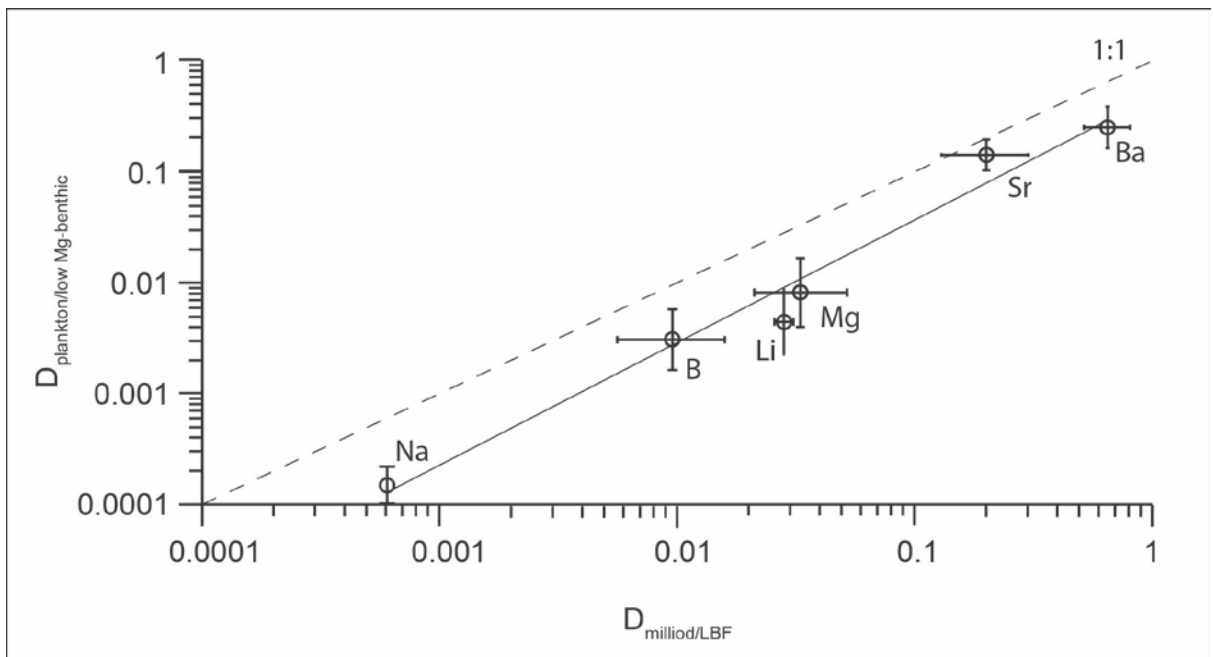
770



771



772



773 **Figure Captions**

774 *Figure 1. Average increase in shell diameter for A. lessonii (left panel) and H. depressa (right*
775 *panel). Dots represent the average of all analysed individuals from one treatment. Error bars*
776 *represent the standard deviation of the mean.*

777

778 *Figure 2. Foraminiferal Ba/Ca as a function of seawater Ba/Ca. Light circles indicate*
779 *individual laser ablation measurements, larger, darker shaded circles represent the average*
780 *Ba/Ca_{cc} for one treatment. Relative standard deviation varies between 16 and 20% for Ba/Ca_{cc}*
781 *in A. lessonii and between 5 and 15% for H. depressa. Average Ba/Ca for the two species*
782 *collected from the aquarium are indicated by triangles (+/- 1 SD) and were not taken into*
783 *account when calculating the regression. Calculated regressions are accompanied by their*
784 *95% confidence intervals (dashed lines) over the Ba/Ca_{sw} range from 50 to 90 μmol/mol. Data*
785 *from Lea and Boyle (1989) is plotted additionally for comparison.*

786

787 *Figure 3. Average (large, darker shaded circles) and single chamber measurements (lighter*
788 *circles) Ba/Ca_{cc}, expressed as their deviation from the mean shell Ba/Ca_{cc} for A. lessonii (left)*
789 *and H. depressa. Error bars represent the standard deviation of the mean, the dashed lines in*
790 *the right panel indicate the 95% confidence intervals for the linear regression.*

791

792 *Figure 4. Relation between the Ba/Ca and Mg/Ca (left panel) and the partition coefficients for*
793 *Ba and Mg (right panel). Every dot represents one single-chamber measurement. The data for*
794 *A. lessonii are indicated by circles, those for H. depressa are represented by open diamonds.*
795 *Every treatment (A-E; Table 1) is indicated by a separate color.*

796

797 *Figure 5: Partition coefficients for Li, B, Na, Mg, Sr and Ba for two groups of foraminifera*
798 *(Large Benthic Foraminifera+Miliolids and the low-Mg species). Data on which the average*
799 *partition coefficients are based, are listed in the online supplement, the ranges indicate the*
800 *maximum range in published partition coefficients. The linear regression between the partition*
801 *coefficients for these two groups is described by: $D_{\text{plankton/low Mg-benthic}}=0.3992*D_{\text{miliolid/LBF}} +$*
802 *0.0081. Elemental results for Miliolid species are confined to Mg/Ca and Sr/Ca. Li/Ca ratios*
803 *were taken from Delaney et al. (1985), Hall and Chan (2004a), Marriott et al. (2004), Yu et al.*
804 *(2005), Ni et al. (2007), Bryan and Marchitto (2008), Hathorne et al. (2009), Dawber and*
805 *Tripati (2012) and Evans et al. (2015); B/Ca ratios are from Yu et al. (2005), Yu and Elderfield*
806 *(2007), Foster (2008), Hendry et al. (2009), Allen et al. (2011; 2012), Dawber and Tripati*
807 *(2012), Babila et al. (2014) and Kaczmarek et al. (2015); Na/Ca are from Delaney et al. (1985),*
808 *Ni et al. (2007), Bian et al. (2009), Wit et al. (2013) and Evans et al. (2015); Mg/Ca are from*
809 *Toyofuku et al. (2000), Raja et al. (2005), Yu et al. (2005), Elderfield et al. (2006), Segev and*
810 *Erez (2006), Hendry et al. (2009), Dueñas-Bohórquez et al. (2009; 2011), Dawber and Tripati*
811 *(2012), Wit et al. (2012; 2013), Babila et al. (2014), De Nooijer et al. (2014a), Sadekov et al.*
812 *(2014) and Evans et al. (2015). Foraminiferal Sr/Ca are taken from Raja et al. (2005), Yu et*
813 *al. (2005), Hendry et al. (2009), Dueñas-Bohórquez et al. (2009; 2011), Dawber and Tripati*
814 *(2012), Wit et al. (2013), De Nooijer et al. (2014a) and Evans et al. (2015). Ba/Ca are from*
815 *this study, Lea and Boyle (1989), Lea and Boyle (1991), Lea and Spero (1994), Hall and Chan*
816 *(2004b), Ni et al. (2007), Hönisch et al. (2011) and Evans et al. (2015).*

817